Physics Letters B 747 (2015) 178–181

Contents lists available at ScienceDirect

Physics Letters B

www.elsevier.com/locate/physletb

Similarities between calculated scission-neutron properties and experimental data on prompt fission neutrons

N. Carjan [a,b,c,*], M. Rizea [b]

[a] Joint Institute for Nuclear Research, FLNR, 141980 Dubna, Moscow Region, Russia
[b] National Institute for Physics and Nuclear Engineering "Horia Hulubei", Str. Reactorului no. 30, P.O. BOX MG-6, Bucharest, Magurele, Romania
[c] CENBG, University of Bordeaux, 33175 Gradignan Cedex, France

ARTICLE INFO

Article history:
Received 1 February 2015
Accepted 19 May 2015
Available online 29 May 2015
Editor: J.-P. Blaizot

Keywords:
Scission neutrons
Prompt neutrons
Dynamical model
Angular distribution
Average energies
Neutron multiplicity

ABSTRACT

The main properties of the neutrons released during the neck rupture are calculated for ^{236}U in the frame of a dynamical scission model: the angular distribution with respect to the fission axis (on spheres of radii R = 30 and 40 fm and at time $T = 4 \times 10^{-21}$ s), the distribution of the average neutron energies (for durations of the neck rupture $\Delta T = 1$ and 2×10^{-22} s) and the total neutron multiplicity (for two values of the minimum neck-radius $r_{min} = 1.6$ and 1.9 fm). They are compared with measurements of prompt fission neutrons during ^{235}U(n_{th}, f). The experimental trends are qualitatively reproduced, i.e., the focusing of the neutrons along the fission axis, the preference of emission from the light fragment, the range, slope and average value of the neutron energy-spectrum and the average total neutron multiplicity.

1. Introduction

The emission of prompt fission neutrons (PFN) is essential in producing nuclear energy since it makes the chain reaction of fissile nuclei possible [1]. The theoretical and experimental study of their properties plays therefore an important role both in the fundamental understanding of the last stage of the fission process and in applications. The main characteristics of PFN (an emission along the fission axis and an exponential decreasing energy spectrum [2,3]) led to the first guess about their origin: they are evaporated by the fission fragments when these fragments are fully accelerated. As a result, we observe a kinematic anisotropy in the laboratory system that originates from an isotropic center of mass (c.m.) emission, the exponential spectrum simply reflecting the fragments' temperature.

The emission is therefore supposed to occur long after the division of the fissioning system into two fragments: it takes $\approx 10^{-20}$ s to reach 90% of TKE and $\approx 10^{-18}$ s to evaporate a neutron if the temperature is ≈ 1 MeV. Comparing to a typical nuclear (Fermi energy) time-scale ($\approx 10^{-22}$ s) these are very long times. One may expect another type of emission to occur before. Moreover, deviations from a standard evaporation spectrum [4–6] or from an isotropic emission in the c.m. [7,8] have been constantly detected. In spite of this, the evaporation hypothesis has never been questioned, its simplicity prevailing any counter argument.

The possibility of an earlier (e.g., around scission) neutron emission of a different origin, that could likewise explain the above mentioned PFN characteristics, was never brought up. However the existence of scission neutrons (SN) was not ignored [9] but they were usually invoked only to explain the deviations (in certain energy or angular domains) from the predictions of the evaporation theory. Such a procedure led obviously to the conclusion that SN represent a small fraction of PFN.

2. Nonadiabatic scission process

The most accepted mechanism for SN emission is the nonadiabatic coupling between the neutron degree of freedom and the rapidly changing neutron-nucleus potential during the scission process i.e., from the neck rupture at finite radius r_{min} to the absorption of the neck stubs by the fragments [10,11]. This idea was recently developed quantitatively in the frame of a quantum-mechanical microscopic model. At the beginning the sudden approximation was used [12–14] assuming the scission process to happen infinitely fast ($\Delta T = 0$). Then the time dependence was introduced through the time-dependent Schrödinger equation (TDSE) with time-dependent potential (TDP) [15,16]. This allows a short but finite transition time ($\Delta T \neq 0$) to be considered. Realistic

* Corresponding author.
E-mail address: carjan@in2p3.fr (N. Carjan).

http://dx.doi.org/10.1016/j.physletb.2015.05.050

values for ΔT are supposed to be around 10^{-22} s. The neutrons present in the fissioning nucleus just before scission evolve in time and quickly find themselves in a postscission potential where they are described by wave packets with some components in the continuum (hence partially released). In this paper we use these unbound parts of the neutron wave packets in order to estimate, for ^{236}U, the angular distribution of the SN with respect to the fission axis, the distribution of the SN average energies and the total SN multiplicity. These estimates are compared with PFN data collected in the thermal-neutron induced fission of ^{235}U.

3. Scission configurations

In our calculations the nuclear shapes just-before scission (two fragments connected by a thin neck) and immediately-after scission (two separated fragments) are described by Cassini ovals [17] with only one deformation parameter: $\alpha_i = 0.985$ (having $r_{min} = 1.6$ fm) and $\alpha_f = 1.001$ (having $d_{min} = 0.6$ fm) respectively. d_{min} is the distance between the surfaces of the two fragments along the z-axes. It is known that these ovals are very close to the conditional equilibrium shapes, obtained by minimization of the deformation energy at fixed value of the distance between the centers of mass of the future fragments [18,19]. To include asymmetric fission it is necessary to introduce a deviation from these ovals defined by a second parameter α_1 [20]. The chosen value of the minimum neck radius (1.6 fm) is slightly lower than predicted by the optimal scission shapes [21]. One can also deduce an approximate neck radius by general considerations like the size of the alpha particle. These theoretical estimates are ≈ 2 fm. Concerning d_{min} one expects to be larger when r_{min} is larger (the restoring forces being in this case stronger) but otherwise d_{min} is unknown.

4. Angular distribution of the unbound neutrons

Let us consider the neutron wave functions after scission (i.e. at $t = \Delta T$) $\hat{\Psi}^i$ (ΔT), that correspond at $t = 0$ to the eigenstates $\hat{\Psi}^i$ that are occupied in the initial configuration α_i. They are numerical solutions of TDSE with TDP obtained as in Refs. [15,16]. Their distribution over the eigenstates of the α_f configuration is given by

$$a_{if} = \langle \hat{\Psi}^i(\Delta T)|\hat{\Psi}^f\rangle. \tag{1}$$

Convention: a wave function that doesn't show a t-dependence is an eigenstate i.e., a solution of the stationary equation. All wave functions have an implicit dependence on the cylindrical coordinates (ρ, z). a_{if} is $\neq 0$ only if $|\hat{\Psi}^i\rangle$ and $|\hat{\Psi}^f\rangle$ have the same projection Ω of the total angular momentum along the symmetry axis.

$f^i = |\hat{\Psi}^i_{em}(t)\rangle$, the emitted part of $|\hat{\Psi}^i(t)\rangle$, is given by the contribution of the unbound states to the wave packet:

$$|\hat{\Psi}^i_{em}(t)\rangle = |\hat{\Psi}^i(t)\rangle - \sum_{\text{bound states}} a_{if}|\hat{\Psi}^f\rangle$$

The corresponding current density weighted by the occupation probability v_i^2 of the respective state i:

$$\bar{D}_{em}(\rho, z) = \frac{i\hbar}{\mu}\sum_i v_i^2(f^i\bar{\nabla} f^{i*} - f^{i*}\bar{\nabla} f^i), \tag{2}$$

provides the distribution of the average directions of motion of the unbound neutrons at any time t.

Here we assume that the fissioning system is in its lowest state at α_i which means a superfluid descent from saddle to just-before scission, i.e. to α_i defined by r_{min}. This is a good approximation in the case of spontaneous or sub-barrier fission [22–25], the partial pair-breaking taking place during the neck rupture.

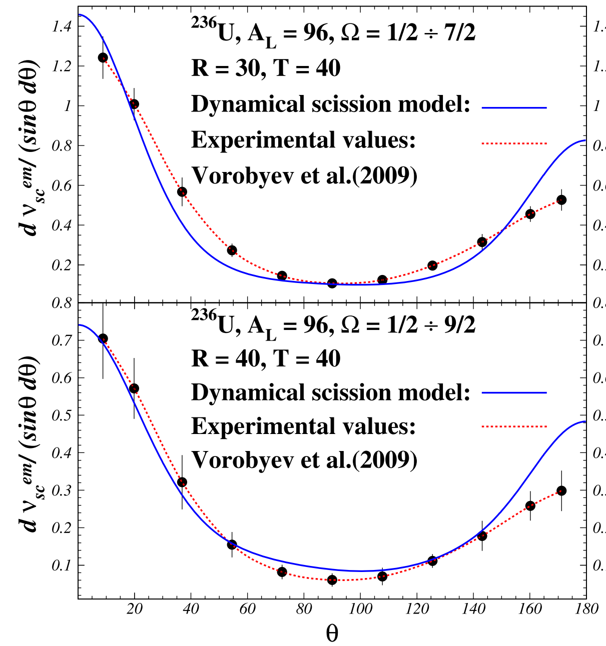

Fig. 1. Comparison between the angular distribution with respect to the fission axis calculated for SN and the one measured for PFN. Calculations are done for the most probable mass ratio $A_L = 96$ on two spheres of radii 30 fm (above) and 40 fm (below). The data points are normalized to the theoretical curve.

To calculate the angular distribution of the SN with respect to the fission axis one needs to integrate in time the radial component of $\bar{D}_{em}$ along the surface of a sphere of radius R containing the fissioning nucleus [26]:

$$d\nu^{em}_{sc}/(\sin\theta d\theta) = 4\pi\int_0^T \bar{D}_{em}(R,\theta,t)\bar{n}(R,\theta)R^2 dt. \tag{3}$$

$\bar{n}$ is the unit vector perpendicular to the surface. For R we choose 30 fm and 40 fm. In the calculations with $R = 40$ fm we also improved the Woods–Saxon potential at scission by replacing the gradient approximation [20] with an exact calculation of the distance to the nuclear surface. The upper limit of the time integral should be in principle ∞. In practice we can reach only a finite value $T = 4 \times 10^{-21}$ s.

The duration of the scission process ΔT is taken 10^{-22} s. During this short time the configuration of the scissioning nucleus is changing drastically from α_i to α_f. For $t > \Delta T$, in first approximation, we freeze the fragments at the configuration α_f since after scission (i.e., after α_f) the neutron motion is much faster than that of just-separated fragments. During this stage, i.e. from $t = \Delta T$ to T, the TDSE is solved neglecting the time dependence of the potential.

Eq. (3) is applied to the most probable mass division ($A_L = 96$) of ^{236}U. To compare with experimental data [27] (that were obtained with 16° angular resolution), the theoretical angular distribution, Eq. (3), has to be folded with the resolution function. The result is shown with solid line in Fig. 1. The resemblance with the measured trend is striking. Calculations with larger radius R and improved scission potential (presented in the lower part of the same figure) bring no significant change.